A Novel Transactive Energy Control Mechanism for Collaborative Networked Microgrids

Weijia Liu, Junpeng Zhan, *Member, IEEE*, and C. Y. Chung, *Fellow, IEEE*

***Abstract* — Collaboration of networked microgrids (NMGs) with diverse generation sources is a promising solution to smooth volatile generation output and enhance the utilization efficiency of renewable energies. In addition to centralized and decentralized collaboration mechanisms, transactive energy control (TEC) is an emerging and effective market-based control to enable energy transactions among distributed entities such as NMGs. However, existing studies on TEC suffer from several major weaknesses such as unconstrained/simplified model formulations and slow convergence rates. This paper proposes a novel TEC mechanism to tackle these weaknesses. First, the centralized mechanism, decentralized mechanism, and subgradient-based TEC mechanism to coordinate the operation of NMGs are briefly reviewed and modeled by a scenario-based stochastic optimization method. A new TEC mechanism is then proposed, consisting of a TEC framework, mathematical model, pricing rule, and algorithm. The optimality of the proposed TEC mathematical model and pricing rule is demonstrated. The effectiveness of the proposed TEC mechanism is verified in case studies where the NMGs operate in grid-connected, islanded, and congested modes. The advantages of the proposed TEC mechanism are also illustrated through comparisons with the centralized mechanism, decentralized mechanism, and subgradient-based TEC mechanism.**

***Index Terms* — Decentralized optimization, electricity market, networked microgrids, renewable energy, transactive energy control**

NOMENCLATURE

Sets and Indices

Ω_K , k	Set and index of scenarios
Ω_M , m	Set and index of MGs
Ω_T , t	Set and index of time slots
$\Psi_{m,k,t}$, j	Set and index of marginal generating units of the m-th MG at time slot t in the k-th scenario
(r)	Index of transaction round

Variables and Parameters

f_E	Energy purchasing cost from external systems
$f_{C,m}$, $f_{U,m}$	Cost and utility functions of the m-th MG
f_S	Cost/benefit function for energy transactions
$\mathbf{h}$	Constraint of the MG interconnection network
$\mathbf{g_m}$	Constraint of the m-th MG
L_m , $L_m^{\oplus}$	Augmented and unaugmented Lagrangians
$P_{E,t}$, $\pi_{E,t}$	Quantity and per-unit price of energy procurement from the external system
$\mathbf{P}_{m,t}^k$	Nodal active power injection vector within the m-th MG in scenario k.
$P_{m,t}^{ex}$, $\pi_{m,t}$	Quantity and per-unit price of active power injection at the substation bus of the m-th MG
$\Delta P_{m,t}^{ex(r)}$	Update of $P_{m,t}^{ex}$ in the r-th transaction round
y , μ	Lagrange multiplier and penalty coefficient of the decentralized algorithm
z , α	Lagrange multiplier of the subgradient algorithm and the step size to update the multiplier
$\varpi_{m,t}$	Coefficient of bid price
$\vartheta_{m,t}$	Locational marginal price at the substation bus of the m-th MG
ζ_e	Error tolerances of bid price
ρ^k	Probability of the k-th scenario

The work was supported in part by Natural Sciences and Engineering Research Council (NSERC) of Canada and the Saskatchewan Power Corporation (SaskPower).

Weijia Liu and C. Y. Chung are with the Department of Electrical and Computer Engineering, University of Saskatchewan, Saskatoon, SK S7N 5A9, Canada (e-mail: liuweijiamarcel@gmail.com, c.y.chung@usask.ca).

Junpeng Zhan is with the Department of Electrical and Computer Engineering, University of Saskatchewan, Saskatoon S7N 5A9, Canada, and also with the Sustainable Energy Technologies Department, Brookhaven National Laboratory, Upton, NY 11973-5000, USA (e-mail: zhanjunpeng@gmail.com)

I. INTRODUCTION

MICROGRIDS (MGs) are widely regarded as a key building block of future smart grid configurations due to their ability to accommodate increasing penetration of distributed energy resources (DERs), including conventional generating units (CGUs), renewable energy sources (RESs), energy storage systems, responsive demands, electric vehicles (EVs), etc. [1], [2]. Meanwhile, the growing integration of distributed RESs with stochastic features challenges the operation of MGs [3], [4]. In recent years, the concept of networked MGs (NMGs), i.e., interconnecting geographically close MGs, has emerged to offer additional operational flexibility and enhance the resilience of existing MGs [5]-[7]. Real-world data from Canada validates that the generation output of geographically adjacent RESs can be diverse and complementary [8], [9]. As such, the collaboration of NMGs is a possible solution to handle the uncertain and volatile generation outputs of RESs and enhance the overall operation efficiency of NMGs.

The collaborative operation of NMGs has been investigated in a number of studies. Methods to address the collaboration of NMGs can be categorized into two mechanisms: centralized [10]-[12] and decentralized [13]-[15]. The centralized mechanism schedules NMGs based on every piece of available information, and thus global optimal solutions can be achieved but at the cost of enormous computational burden and privacy concerns [16]. The decentralized mechanism is capable of finding satisfactory solutions while protecting crucial information of individual MGs; however, the interconnection network among NMGs cannot be monitored by individual MG operators, and thus the optimized solutions might not meet the requirement of secure NMG operation [4].

As an efficient method to allocate resources and coordinate operations among different MGs, transactive energy control (TEC) shows promise for integrating a vast number of RESs and responsive devices in the smart grid context [17], [18]. TEC is a market-based distributed mechanism that coordinates multiple resources/entities based on bidirectional communication. Instead of the exchange of information that lacks explicit physical meaning, which occurs in most existing decentralized mechanisms, TEC is able to make decisions based on the exchange of value-based information (electricity price signals for power system applications) [17]. Thus, individual NMGs are able to express their preferences for collaboration through exchanged price signals within the TEC framework.

TEC generally solves the collaborative operation of NMGs through iterative information exchange-based methods [18]. A number of studies have been conducted in recent years on the implementation of TEC and energy trading in power system areas. Dual decomposition-based TEC is employed in [18] to coordinate EV aggregators and the distribution system operator in congestion management. A Nash bargaining formulation for energy trading among NMGs is proposed in [19], and the proposed model is decomposed and solved by the alternating direction method of multipliers (ADMM). An “internal price” concept is developed in [20] to coordinate the energy sharing among MGs, where the prosumers submit their desired energy and react to the broadcasted price signals. The energy trading of NMGs is formulated as an unconstrained Stackelberg game in [21], and equilibrium is achieved through relaxation algorithms. Peer-to-peer energy trading models considering the preferences of prosumers are proposed in [22] and the trading price is approached by ADMM. Locational marginal pricing (LMP) is utilized to motivate the energy transactions among MGs in [23], and the energy transactions are solved by an auction process. In [24], price-responsive DERs are described by linear demand-price curves and model predictive control is employed to solve the aggregated model of DERs under transactive coordination. A market-based multi-agent TEC for EV charging is proposed in [25], where the equilibrium prices are approached by a trial-and-error process. A dual subgradient algorithm is utilized to coordinate the operation of MGs in [26] and [27], while the TEC mechanisms studied are simplified to consider unconstrained generation profiles and power flows. Double auction-based TEC for EVs and MGs are respectively discussed in [28] and [29], where the bid prices of local entities are optimized through unconstrained models.

In summary, existing studies on TEC have not comprehensively considered the physical constraints of power networks. The constraints of power networks are either ignored (e.g., [18]-[22], [26]) or simplified (e.g., [23]-[25], [27]-[29]). Moreover, the decentralized ADMM algorithm and dual subgradient algorithm are widely used to decouple and solve the TEC models. Consequently, the following weaknesses of these studies for coordinating the operation of NMGs are identified:

- The application of existing TEC is strictly limited due to the absence of physical operational constraints such as power flow constraints, e.g., existing TEC cannot properly deal with transmission/distribution congestion and might lead to infeasible solutions.
- In ADMM and subgradient algorithms, the Lagrangian multipliers are updated/approached with constant or diminishing step sizes, which do not provide explicit market information or reflect the preferences of TEC participants in collaboration. Moreover, the commonly used subgradient algorithm has poor convergence properties, including strict convergence criteria and a slow convergence rate [30].

This paper develops a novel TEC mechanism that consists of a TEC framework, mathematical model, pricing rule, and algorithm to coordinate the day-ahead collaboration among NMGs. The physical constraints of power system operation are comprehensively considered and integrated into the proposed models to account for loss, congestion, and voltage. In the proposed TEC mechanism, the operators of individual MGs optimize its daily schedules and submit bid prices to a system coordinator. The system coordinator clears the energy bids and allocates the energy inputs/outputs to different MG operators. Different from the framework in [19]-[21] where the MGs respond to the prices provided by the system coordinator, the MG operators of the proposed TEC instead submit their preferences in the forms of bid prices to the system coordinator. The proposed TEC mechanism overcomes the aforementioned weaknesses in the following ways:

- The first weakness is handled by integrating physical operating constraints of both the individual MGs and the MG interconnection network into the proposed TEC models. The MG operators optimize their day-ahead operating schedules, and the system coordinator monitors the status of the interconnection network among MGs and verifies the feasibility of energy transactions. In this way, the proposed TEC mechanism is applicable to NMGs in grid-connected, islanded, and congested modes and the optimized solution is demonstrated to be equivalent to that obtained from the centralized mechanism.
- An iterative auction procedure is employed, and a new pricing rule is developed for individual MG operators to formulate optimal bid prices to tackle the second weakness. The pricing rule developed is not approached by the subgradient-based algorithm and is derived from the concept of LMP, which provides explicit market information and illustrates the preferences of individual MGs participating in energy transactions.

The remainder of this paper is organized as follows. Section II discusses the NMG collaboration framework, uncertainty modeling, and assumptions adopted in this paper. Section III briefly reviews the centralized mechanism, ADMM-based decentralized mechanism, and subgradient-based TEC mechanism with respect to promoting the collaborative operation of NMGs. Section IV proposes a new TEC mechanism and demonstrates the optimality and effectiveness of the proposed mathematical model and pricing rule. Section V provides numerical test results to verify the effectiveness of the proposed TEC mechanism in dealing with grid-connected, islanded, and congested NMGs. Finally, Section VI concludes the paper.

II. NMG Collaboration Framework

A. Illustrative Example of NMG Collaboration Framework

Generally, NMGs consist of a number of MGs that have clearly defined electrical boundaries between them and an interconnection network connecting them. A typical topology of NMGs is illustrated in Fig. 1, where each MG may consist of power loads, CGUs, and RESs. In this paper, the emphasis is laid on the collaboration of NMGs through scheduling the generation outputs of CGUs and RESs.

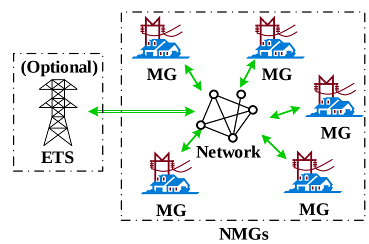

Fig. 1. A typical topology of NMGs.

Note that support from the external transmission system (ETS) is only available to grid-connected NMGs. Nonetheless, the collaborative mechanism should be effective for both grid-connected and islanded NMGs. Without loss of generality, the NMG collaboration mechanisms are established based on grid-connected NMGs in this paper. Islanded NMGs are modeled by constraining the power flow between the ETS and the NMGs to zero. To guarantee the feasibility of coordinated operation among NMGs, i.e., the solution to the operation of NMGs exists, load shedding or RES curtailment shall be implemented if necessary.

There are two categories of entities in the framework studied: MG operators and the system coordinator. Basically, the role of each MG operator is to manage the operation of the resources and distribution network within its control, while the system coordinator manages the operation of the MG interconnection network and serves as an interface between the NMGs and the utility grid (e.g., ETS in Fig. 1), as described in [19]-[21]. However, the responsibilities and privileges of the system coordinator may vary with the NMG collaboration mechanisms, which will be further explained in Sections III and IV.

B. Uncertainty Modelling

Typically, the operation of NMGs is affected by a number of uncertainty factors, including RES generation, load consumptions, market price, etc. Among them, the intermittent nature of RES generation has the most significant influence on the feasibility of NMG operation and collaboration. In this paper, the uncertainty of RES generation output is modeled by a scenario-based stochastic optimization method proposed in [31]. The scenario-based stochastic optimization method can be extended to accommodate other uncertain factors such as the fluctuations of loads and energy prices; however, this will not be further discussed as this paper focuses on the collaboration of CGUs and RESs. The NMG collaboration mechanisms in this paper are established based on the scenario-based stochastic optimization. If only one scenario is considered, the proposed models will automatically degrade to deterministic models. The deterministic and stochastic models are further compared in case studies.

C. General Assumptions

The following two assumptions are adopted in this paper:

(i) Each MG can be described by a number of radial distribution networks.

(ii) The objective functions of individual MGs can be described by quadratic functions.

Assumptions (i) and (ii) are widely used in existing research to model the distribution networks and the objective function of system operators, such as in [13] and [16], respectively. Thus, the introduction of these assumptions does not hinder the feasibility and effectiveness of NMG collaboration models and methods proposed in this paper.

III. Existing Collaborative Mechanisms for NMGs

A. Centralized Mechanism

A diagram of the centralized collaboration mechanism of NMGs is given in Fig. 2. The system coordinator functions as a system operator who is in charge of the operation of both the NMGs and the interconnection network. All the resources in the NMGs will be centrally dispatched by the system coordinator based on all the data from the NMGs and interconnection network. The MG operator, on the other hand, will strictly follow the schedules optimized by the system coordinator.

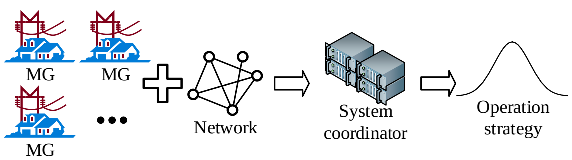

Fig. 2. Centralized operation of NMGs.

The operation objective of the central system coordinator is to maximize the social welfare of all NMGs. The scenario-based centralized NMG collaboration model is discussed in detail in Appendix A. The constraints include the AC power flow equations (A2)-(A5), generation output and ramping limits of generating units (A6)-(A8), line capacity limit (A9), and voltage magnitude limit (A10). For the sake of simplicity, the centralized NMG collaboration model is denoted as M1 and described as follows:

(M1)

$$\min_{P_{E,t},P_{m,t}^{ex},\mathbf{P}_{m,t}^{k}} \sum_{t\in\Omega_T}\sum_{k\in\Omega_K}\sum_{m\in\Omega_M} \rho^k\left(f_{C,m}(\mathbf{P}_{m,t}^{k})-f_{U,m}(\mathbf{P}_{m,t}^{k})\right) + \sum_{t\in\Omega_T} f_E(P_{E,t}) \tag{1}$$

$$\text{s.t.} \quad \mathbf{h}(P_{m,t}^{ex},P_{E,t})=\mathbf{0} \tag{2}$$

$$\mathbf{g}_m(P_{m,t}^{ex},\mathbf{P}_{m,t}^{k})=\mathbf{0},\ \forall k\in\Omega_K,\ \forall m\in\Omega_M \tag{3}$$

where the objective function (1) maximizes the social welfare of all NMGs. Note that the nodal power injection vector $\mathbf{P}_{m,t}^{k}$ is influenced by the RES generation output scenarios, while $P_{E,t}$ and $P_{m,t}^{ex}$ do not depend on scenarios so that a robust decision in day-ahead energy market can be made before the realization of any one of the scenarios [31]. The constraints have been decomposed into two modules, namely the constraints of the interconnection network (2) and the constraints of individual MGs (3). In this paper, model M1 is expressed in the slack form, where constraints (2) and (3) are represented as equality constraints. This is achieved by introducing non-negative slack variables to inequality constraints (A6)-(A10) [32].

However, model M1 is a non-convex nonlinear model. Based on assumption (i), the nonlinear constraints $\mathbf{g}_m$ of the m-th MG can be relaxed through the convex second-order cone (SOC) relaxation method proposed in [13], [14], and [33], which will not be further discussed in this paper. In existing literature, $\mathbf{h}$ is normally linearized ignoring the voltage and loss information such as demonstrated in [23]. In this paper, the method proposed in [34] is adopted to linearize $\mathbf{h}$ while maintaining accurate approximations of voltage magnitudes and transmission losses. The linearization of $\mathbf{h}$ is briefly described in Appendix B.

By linearizing $\mathbf{h}$, relaxing $\mathbf{g}_m$ with the SOC method, and considering assumption (ii), M1 becomes a convex quadratically constrained quadratic programming model, which can be further converted into a convex SOC programming model and solved by commercial solvers. Note that the physical constraints of AC power systems have been properly considered in both the relaxation of $\mathbf{g}_m$ and the linearization of $\mathbf{h}$. Thus, the solution to model M1 is able to provide information such as voltage magnitudes, line losses, and congestion.

B. Decentralized Mechanism

In M1, the interconnection network is constrained by (2), while the operation of each MG is constrained by (3). Thus, it is possible to solve M1 in a decentralized manner.

In the decentralized mechanism, a system coordinator is not required. Each MG operator is responsible for optimizing its individual operation strategy based on information of its own demand and resources and the shared knowledge of other MGs. The shared knowledge will be exchanged and updated based on predefined protocols. A diagram of the decentralized operation of NMGs is provided in Fig. 3.

In this paper, the ADMM is adopted to decompose M1 into individual operation models of MGs [35]. For the m-th MG, the augmented Lagrangian L_m can be written as:

$$L_m(P_{m,t}^{ex},P_{E,t},y)=\sum_{t\in\Omega_T}\sum_{k\in\Omega_K}\rho^k\left(f_{C,m}(\mathbf{P}_{m,t}^{k})-f_{U,m}(\mathbf{P}_{m,t}^{k})\right) + \sum_{t\in\Omega_T} f_E(P_{E,t}) + y^{\mathrm{T}}\mathbf{h}(P_{m,t}^{ex},P_{E,t}) + \frac{\mu}{2}\left\|\mathbf{h}(P_{m,t}^{ex},P_{E,t})\right\|_2^2 \tag{4}$$

where $\|\ \|_2$ denotes the Euclidean norm.

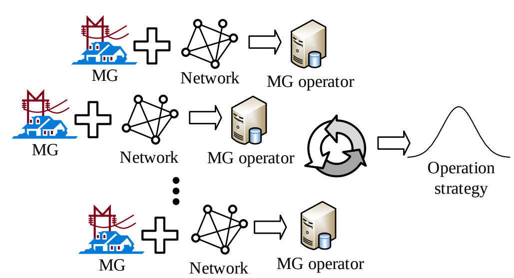

Fig. 3. Decentralized operation of NMGs.

The model of the decentralized operation mechanism for the m-th MG, denoted as M2, can be formulated as:

(M2)

$$\min_{P_{E,t},P_{m,t}^{ex},\mathbf{P}_{m,t}^{k}} L_m(P_{m,t}^{ex},P_{E,t},y) \tag{5}$$

$$\text{s.t.} \quad (3)$$

The update rule of the ADMM is not discussed further; details can be found in [30]. To guarantee the optimality and convergence of the ADMM, the SOC relaxed $\mathbf{g}_m$ should be further relaxed based on [36] to achieve a zero duality gap, the details of which are described in Appendix B. In summary, the optimality and convergence of ADMM-based model M2 are guaranteed, i.e., M1 and M2 have the same optimal solution.

C. Subgradient-based TEC Mechanism

The subgradient-based TEC mechanism is similar to the decentralized mechanism described in Fig. 3. However, the constraint $\mathbf{h}$ is integrated to the objective of the m-th MG through an unaugmented Lagrangian $L_m^{\oplus}$, as described in (6):

$$L_m^{\oplus}(P_{m,t}^{ex}, P_{E,t}, z) = \sum_{t\in\Omega_T}\sum_{k\in\Omega_K} \rho^k (f_{C,m}(\mathbf{P}_{m,t}^k) - f_{U,m}(\mathbf{P}_{m,t}^k))) + \sum_{t\in\Omega_T} f_E(P_{E,t}) + z^{\mathrm{T}}\mathbf{h}(P_{m,t}^{ex}, P_{E,t}) \tag{6}$$

The mathematical models of the subgradient-based TEC mechanism, denoted as M3, can be formulated based on unaugmented Lagrangian $L_m^{\oplus}$ as:

$$\textbf{(M3)} \quad \min_{P_{E,t}, P_{m,t}^{ex}, \mathbf{P}_{m,t}^k} L_m^{\oplus}(P_{m,t}^{ex}, P_{E,t}, z) \quad \text{s.t. (3)} \tag{7}$$

The Lagrange multiplier z is updated based on the selected step size α as shown in (8):

$$z = z + \alpha \mathbf{h}(P_{m,t}^{ex,u}, P_{E,t}^u) \tag{8}$$

In fact, the subgradient-based TEC model M3 is intrinsically a decentralized model based on an unaugmented Lagrangian. Compared to the ADMM-based model M2, which introduces the augmented Lagrangian (i.e., the Euclidean norm in (4)) to improve the convergence properties, the subgradient-based model M3 suffers from a number of disadvantages [37]:

- Strict convergence criteria: M3 only converges at an appropriate step size α and exceptional conditions, e.g., objectives must be strictly convex [16].
- Poor convergence properties: M3 has a very slow convergence rate and might lead to unbounded solutions, which have already been observed in existing studies such as [27].

IV. A Novel Transactive Energy Control Mechanism

The decentralized mechanism and subgradient-based TEC mechanism decompose the centralized model M1 based on Lagrangian relaxation. However, consideration of the interconnection network (i.e., constraint (2)) in objective functions (5) and (7) is beyond the scope of individual MG operators, i.e., individual MG operators are only responsible for the operation of MGs under their control. To ensure the feasible and reasonable implementation of TEC, a novel TEC mechanism is proposed in this section to achieve efficient collaboration among NMGs.

A. The Framework of Proposed TEC

Unlike the decentralized model M2 and subgradient-based model M3, the proposed TEC mechanism requires a system coordinator to manage the energy transactions among NMGs. However, the role of the system coordinator in the proposed TEC mechanism is also different from that in centralized model M1. In M1, the role of the system coordinator is more like a utility grid operator who is responsible for scheduling all the resources in both the interconnection network and individual MGs. In contrast, the role of the system coordinator in the proposed TEC is similar to an independent operator in electricity markets who only manages the energy trading through the interconnection network. Thus, the privacy of individual MGs is protected since the system coordinator in the proposed TEC mechanism does not have access to the data of individual MGs. The responsibilities and privileges of the system coordinator in the centralized and proposed TEC mechanisms are compared in Table I.

The individual MG operators and system coordinator will interact through bidirectional communication to achieve the efficient scheduling of resources in NMGs. Within the framework of the proposed TEC, individual MG operators submit price bids to the system coordinator with their preferences to trade energy among various MGs, while the system coordinator optimizes the allocation of the bids received and provides feedback regarding successful energy transactions. An iterative auction procedure is adopted so that the MGs can modify their participating strategies according to the successful energy transactions and update their bids until satisfactory results have been achieved. The proposed TEC is illustrated in Fig. 4.

TABLE I
RESPONSIBILITIES AND PRIVILEGES OF THE SYSTEM COORDINATOR IN THE CENTRALIZED AND PROPOSED TEC MECHANISMS

	Centralized	Proposed TEC
Constraints of system coordinator	(2) and (3)	(2)
System coordinator's knowledge of individual MGs	All data	Price submitted by individual MGs

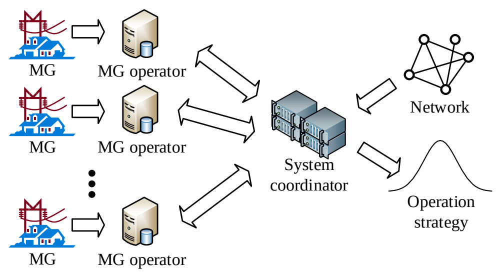

Fig. 4. The proposed TEC of NMGs.

B. Mathematical Model of Proposed TEC

Based on Fig. 4, two mathematical models (namely M4-MG and M4-S) are formulated for individual MG operators and the system coordinator, respectively. M4-MG and M4-S together formulate the complete TEC model, which is denoted as M4.

Different from Lagrangian relaxation-based M2 and M3, a cost/benefit function of energy transactions, denoted as f_S, is introduced to charge/reward individual MGs based on $P_{m,t}^{ex}$. In addition, f_S is properly designed such that an MG is charged/paid for purchasing/selling energy. In this paper, the M4-MG model for the m-th MG aims to minimize the total procurement cost or maximize the social welfare. M4-MG can be expressed as:

$$\textbf{(M4-MG)} \quad \min \sum_{k\in\Omega_K}\sum_{t\in\Omega_T} \rho^k (f_{C,m}(\mathbf{P}_{m,t}^k) - f_{U,m}(\mathbf{P}_{m,t}^k)) + \sum_{t\in\Omega_T} f_S(P_{m,t}^{ex}) \quad \text{s.t. (3)} \tag{9}$$

Accordingly, the M4-S model for the system coordinator aims to minimize the energy procurement from ETS (if available) and maximize the social welfare of energy transactions among NMGs. M4-S can be expressed as:

$$\textbf{(M4-S)} \quad \min \sum_{t\in\Omega_T} f_E(P_{E,t}) - \sum_{t\in\Omega_T}\sum_{m\in\Omega_M} f_S(P_{m,t}^{ex}) \quad \text{s.t. (2)} \tag{10}$$

In this paper, f_E and f_S are assumed to be proportional to the quantities of energy transactions:

$$f_E(P_{E,t}) = \pi_{E,t} P_{E,t} \tag{11}$$

$$f_S(P_{m,t}^{ex}) = -\pi_{m,t} P_{m,t}^{ex} \tag{12}$$

Based on the formulation of M4 and the characteristics of f_E and f_S discussed in (11) and (12), the proposed TEC will guarantee that the optimal solution of M4 is equivalent to that of M1. The optimality of M4 can be derived as follows.

Theorem 1: The bid price $\pi_{m,t}$ exists for MG operators such that the optimal solution to model M4 is equivalent to the optimal solution to model M1.

The proof of Theorem 1 is provided in Appendix C. Note that the optimal solution to the proposed TEC model M4 is also the optimal solution to the centralized model M1, so solving M4 is equivalent to solving M1. Thus, the proposed TEC model is able to deal with operating issues such as congestion and uncertainty when coordinating the operation of NMGs.

C. Pricing Rule

Theorem 1 proves that it is possible to construct a price $\pi_{m,t}$ that makes solving the proposed TEC model M4 equivalent to solving model M1. To achieve this efficient allocation, it is necessary to construct a pricing rule to update $\pi_{m,t}$. Based on the formulation of M4, an optimal pricing rule to construct and update $\pi_{m,t}$ is proposed in this subsection.

As illustrated in Fig. 4, the proposed TEC will proceed through an iterative auction process. If the successful energy transaction of the *m*-th MG at the *r*-th round bidding is $\Delta P_{m,t}^{ex(r)}$, then the accumulated successful energy transaction in the first *r* rounds, denoted as $P_{m,t}^{ex(r)}$, can be calculated as:

$$P_{m,t}^{ex(r)} = P_{m,t}^{ex(r-1)} + \Delta P_{m,t}^{ex(r)} \tag{13}$$

Based on the formulation of f_S proposed in (12) and the updating rule of $P_{m,t}^{ex}$ in (13), the *r*-th round bid price of the *m*-th MG, denoted as $\pi_{m,t}^{(r)}$, is constructed as follows:

$$\pi_{m,t}^{(r)} = \varpi_{m,t}\Delta P_{m,t}^{ex(r)} + \vartheta_{m,t}^{(r-1)} \tag{14}$$

In each transaction round, each MG operator submits $\varpi_{m,t}$ and $\vartheta_{m,t}^{(r-1)}$ to the system coordinator for transaction clearing. Note that $\varpi_{m,t}$ and $\vartheta_{m,t}^{(r-1)}$ are both derived from the concept of LMP. In this paper, $\vartheta_{m,t}^{(r-1)}$ and $\varpi_{m,t}$ are calculated as follows:

- $\vartheta_{m,t}^{(r-1)}$ can be obtained from the *m*-th MG operator by solving M4-MG model based on $P_{m,t}^{ex(r-1)}$. In the first transaction round ($r=1$), each MG operator solves M4-MG with $P_{m,t}^{ex(0)}=0$. If $r>1$, each MG operator solves M4-MG based on the successful transactions $P_{m,t}^{ex(r-1)}$ in the first $r-1$ rounds. The marginal price $\vartheta_{m,t}^{(r-1)}$ is obtained from the solution of M4-MG.
- $\varpi_{m,t}$ can be calculated based on the cost coefficients of marginal generating units of the *m*-th MG. If the generation output of a generating unit has not reached its upper/lower limits and ramping limits (i.e., constraints (A6)-(A8) in Appendix A are non-binding and the dual variables of (A6)-(A8) equal zero), this generating unit is defined as a marginal unit. Three possible cases are identified: 1) at least one CGU is a marginal unit; 2) all marginal units are RESs; and 3) no generating unit is marginal. Let α_j^k denote the leading coefficient of the quadratic cost/utility function of the *j*-th marginal generating unit in the *k*-th scenario, and $\Psi_{m,k,t}$ denote the set of marginal generating units within the *m*-th MG at time slot *t* in the *k*-th scenario. $\varpi_{m,t}$ is calculated as follows:

$$\varpi_{m,t} = \sum_{k\in\Omega_K}\rho^k\Big(\sum_{j\in\Psi_{m,k,t}}\frac{1}{\alpha_j^k+\varepsilon}\Big)^{-1} \tag{15}$$

where ε is a very small positive value (1e-6 in this paper). In case 1), $\varpi_{m,t}$ is affected by α_j^k of marginal CGUs and ε does not affect the result because it is too small. In both cases 2) and 3), no CGU is marginal and α_j^k equals to zero. According to (15), $\varpi_{m,t}$ equals ε and is further regarded as zero in these two cases. This is in line with the fact that the cost increments of the *m*-th MG in cases 2) and 3) are not relevant to the cost functions of CGUs within the *m*-th MG.

Theorem 2: The pricing rule proposed in (14) is the optimal bidding price for NMGs based on the proposed TEC model.

The proof of Theorem 2 is provided in Appendix D. In summary, the TEC will proceed through an iterative auction process as described by Algorithm 1.

Algorithm 1

1. Initialize the convergence error tolerance ζ_e, set $P_{m,t}^{ex(0)}=0$.
2. In the *r*-th round bidding, each MG operator solves its individual M4-MG model based on $P_{m,t}^{ex(r-1)}$. Based on the optimal solution to the M4-MG model, the bid information $\varpi_{m,t}$ and $\vartheta_{m,t}^{(r-1)}$ will be updated and submitted to the system coordinator based on the pricing rule (14).
3. The system coordinator solves the M4-S model based on the $\varpi_{m,t}$ and $\vartheta_{m,t}^{s(r-1)}$ received, and announces the successful transactions $\Delta P_{m,t}^{ex(r)}$ to MG operators.
4. If *r*>1 and the stopping criterion (16) is met, the energy transactions are considered converged and go to step 5. Otherwise, repeat steps 2-4 with $r=r+1$.
$$\left\|\pi_{m,t}^{(r)}-\pi_{m,t}^{(r-1)}\right\|_2^2 \le \zeta_e \tag{16}$$
5. Output: $P_{m,t}^{ex}$, $\mathbf{P}_{m,t}^{k}$, $\pi_{m,t}$

D. Comparison of NMG Collaboration Mechanisms

The characteristics of the centralized mechanism, decentralized mechanism, subgradient-based TEC mechanism, and proposed TEC mechanism are compared in Table II. The performance of these mechanisms is further compared in Section V.

TABLE II
COMPARISON OF NMG COLLABORATION MECHANISMS

	M1	M2 & M3	M4
System coordinator	Required	None	Required
System coordinator's knowledge of NMGs	Full	N/A	Limited
Privacy of NMGs	Not protected	Protected	Protected
NMGs' knowledge of interconnection network	None	Full	None
Data exchange among NMGs	None	Limited	None
Model scale	Global	Local	Local
Iteration	Not required	Required	Required

V. CASE STUDY

A. Case Study Setup

A test system as illustrated in Fig. 5 is employed for the case study. A total of five MGs are included, and the IEEE 123 bus distribution system with a peak load capacity of 3.8 MW is applied to each MG. Four MG operators are considered, as MG_4 and MG_5 are considered as one MG entity (denoted as MG-4). The operation horizon considered is 24 hours, and the time resolution is set to 15 minutes (96 time slots in total). RES curtailment and load shedding are integrated into the proposed model by modifying power injection constraints and adding curtailment/shedding penalties to the operation objective functions. The penalty for renewable curtailment or load shedding is set to \$50/MWh, which is much higher than the average energy procurement price from ETS (\$10.8/MWh). The setup of the generating units in the MGs can be found in Table III. The convergence criteria for models M2, M3, and M4 are all set to 1e-6, and the step sizes of M2 and M3 are set to 0.1. The proposed algorithms are coded with CPLEX 12.7, which was run on a desktop computer with Intel i7 processors and 12 GB memory.

The wind and solar generation outputs are both derived from real measured data from Canada [8], [9]. Three RES generation scenarios are considered namely central forecast, high forecast, and low forecast, with probabilities of 0.6, 0.2, and 0.2, respectively, as per [31], [38], and [39]. For simplicity, the high and low forecasts are respectively 120% and 80% of the value of the corresponding central forecast, and these three scenarios are regarded as the representative scenarios after scenario generation and reduction. The determination of representative scenarios can refer to [40] but is not discussed in detail in this paper. Note that the number of scenarios does not hinder the effectiveness of the proposed TEC mechanism in uncertainty modeling. Moreover, RES data from June 30 and December 31, 2008, are selected to represent the operation of NMGs on a summer day (SD) and a winter day (WD), respectively.

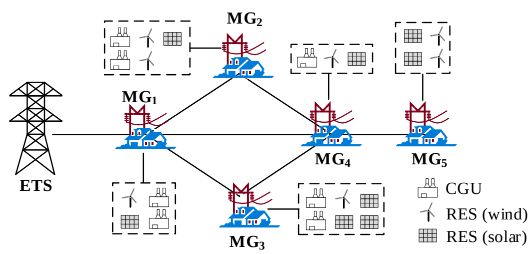

Fig. 5. The topology of a test system with five MGs and four MG entities.

TABLE III
PARAMETERS OF GENERATING UNITS IN NMGS

MG entity	MG	Number of CGUs	Total rated power of CGUs	Number of RESs	Total rated power of RESs
MG-1	MG_1	2	3.3 MW	2	1.8 MW
MG-2	MG_2	2	3.6 MW	3	3.0 MW
MG-3	MG_3	2	3.3 MW	4	4.0 MW
MG-4	MG_4	1	1.5 MW	2	1.8 MW
	MG_5	0	N/A	4	4.2 MW

In addition to the SD and WD, the following terms used in the case studies are specifically defined as follows: 1) *collaborative*: NMGs collaborate with each other; 2) *non-collaborative*: NMGs do not collaborate with each other; 3) *deterministic*: only the central forecast is employed; 4) *stochastic*: all the scenarios are considered; 5) *grid-connected*: the NMGs are connected to the ETS; 6) *islanded*: the NMGs are disconnected from the ETS; and 7) *congested*: the NMG interconnection network and individual MGs may suffer from congestion.

Notably, the subgradient-based TEC model M3 fails to converge in most simulation cases, and thus the results are not provided in Sections V-B and V-C. Instead, the performance of M3 is discussed in Section V-D.

B. Deterministic Operation Results

This subsection aims to validate the effectiveness of the proposed TEC model M4 in dealing with deterministic collaboration of NMGs in grid-connected, islanded, and congested modes.

First, collaborative and non-collaborative modes of grid-connected NMGs are compared to validate the necessity of collaboration among NMGs. The day-ahead operation results and costs are compared in Table IV. Compared to non-collaborative NMGs, the collaborative NMGs import less energy from the ETS and generate more electricity from their RESs and CGUs. By trading power generated at lower costs among NMGs, the total daily operating costs are reduced by 16.4% and 1.4% on the SD and WD, respectively. Collaboration creates more benefits in the SD because it reduces the RES curtailment, which is further illustrated in Fig. 6. In Fig. 6, the generation outputs of RESs and CGUs in MG-3 on the SD are taken as an example. In the non-collaborative mode, MG-3 must curtail the generation of RESs during late night and noon periods. In the collaborative mode, however, RES generation capabilities can be fully utilized as MG-3 is able to trade its excess RES generation to other MGs. In addition, the generation output of CGUs is significantly higher in the collaborative mode as the generation capabilities of CGUs whose generating costs are lower than that of ETS can be traded among NMGs. In this case, the other MGs are able to reduce their energy procurement costs, and the total costs of all the NMGs will decrease as shown in Table IV. Thus, the collaboration of NMGs is beneficial.

To achieve optimal collaboration among NMGs, the performance of models M1, M2, and M4 is compared in Table V. The total operating cost is considerably higher in the winter due to the decline in solar generation. If the optimal solution of M1 is selected as the benchmark, the relative errors of daily energy costs based on the proposed TEC mechanism are only 0.05% and 0.01% on the SD and WD, respectively. Table VI lists the operation results of NMGs operating in islanded mode and shows that the lack of RES generation on the WD will lead to load shedding for islanded NMGs. The costs of load shedding based on M2 and M4 are identical and slightly higher than that based on M1. Similar to the results of grid-connected NMGs, the daily costs of different mechanisms are close to one another.

TABLE IV
COMPARISON OF GRID-CONNECTED NMGS IN COLLABORATIVE AND NON-COLLABORATIVE MODES

	Non-collaborative		Collaborative	
	SD	WD	SD	WD
Daily RES generation (MWh)	161.0	89.2	162.8	89.2
Daily RES curtailment (MWh)	1.8	0.0	0.0	0.0
Daily import from ETS (MWh)	47.4	96.3	18.3	80.9
CGU generation (MWh)	104.4	127.2	131.8	142.3
RES curtailment cost ($)	90.0	0.0	0.0	0.0
Daily total cost ($)	1346.1	2062.3	1156.1	2033.2
Collaborative cost reduction (%)	--	--	16.4	1.4

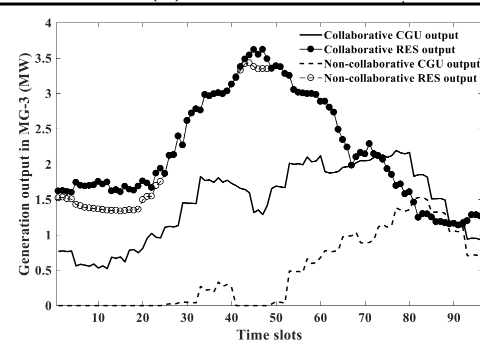

Fig. 6. Comparison of collaborative and non-collaborative RES and CGU generation curves for MG-3 on the SD.

TABLE V
DAILY ENERGY COSTS ($) OF GRID-CONNECTED NMGS

Model	SD	WD
M1	1156.1	2033.2
M2	1156.6 (0.04%)	2033.5 (0.01%)
M4	1156.7 (0.05%)	2033.5 (0.01%)

*values in brackets indicate the relative error compared to benchmark results based on model M1.

TABLE VI
DAILY COSTS ($) OF ISLANDED NMGS

	M1	M2	M4
SD daily energy cost	1174.5	1175.1	1174.8
SD load shedding cost	0.0	0.0	0.0
SD total cost	1174.5	1175.1 (0.05%)	1174.8 (0.03%)
WD daily energy cost	1970.2	1969.5	1969.5
WD load shedding cost	675.5	689.5	689.5
WD total cost	2645.7	2659.0 (0.50%)	2659.0 (0.50%)

*values in brackets indicate the relative error compared to benchmark results based on model M1.

The daily overall energy transactions through the MG interconnection network in grid-connected and islanded modes are compared in Fig. 7. The daily overall energy transactions are calculated by summing up the transactive energy of each 15-minute time slot. The energy transactions among NMGs operating in grid-connected mode and islanded mode demonstrate significant differences on the WD due to the insufficient power generation capacity, while the differences on the SD are relatively smaller.

The computational burdens of M1, M2, and M4 (M4-MG and M4-S combined) when solving grid-connected and islanded NMGs are compared in Table VII. The proposed M4 and ADMM-based M2 require a comparable number of iterations to converge for grid-connected NMGs, but the proposed M4 converges much faster than M2 for islanded NMGs, especially on the WD when load shedding becomes inevitable. The proposed TEC mechanism takes the least amount of computational time because M4-MG model is a parallel process model, while the ADMM-based model M2 takes the longest because it is solved in a sequential manner. The convergence properties of M2 and M4 for grid-connected NMGs are demonstrated in Fig. 8. In Fig. 8, the calculation of the primal and dual errors of the ADMM algorithm can be found in [34], and the bid price error is obtained from (16). Note that the convergence error tolerances are set to 1e-6 in these studies. If the convergence error tolerances are relaxed to 1e-4 (acceptable in most cases), the computational burdens of M2 and M4 for the grid-connected NMGs will significantly decrease as M2 and M4 will converge after 19 (11) and 14 (15) iterations on the SD (WD), respectively.

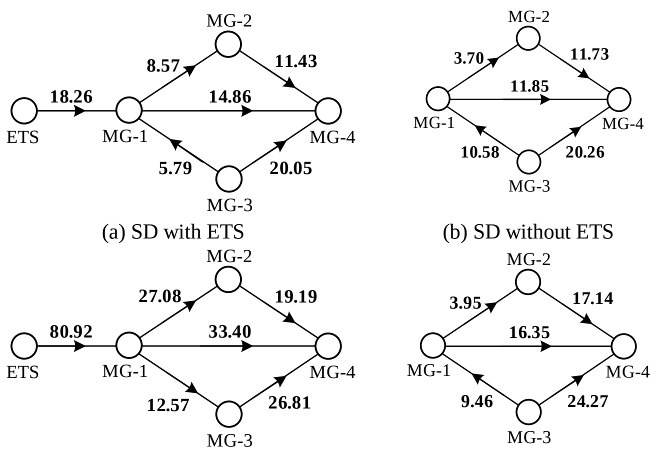

(a) SD with ETS (b) SD without ETS

(c) WD with ETS (d) WD without ETS

Fig. 7. Profile of daily overall energy transactions among NMGs in MWh.

TABLE VII
COMPUTATIONAL PERFORMANCE IN TERMS OF ITERATIONS AND TIME OF DIFFERENT MECHANISMS

	M1	M2	M4
Grid-connected iterations to converge on SD	1 (403)	23 (773)	29 (197)
Grid-connected iterations to converge on WD	1 (387)	19 (527)	18 (108)
Islanded iterations to converge on SD	1 (389)	27 (818)	13 (85)
Islanded iterations to converge on WD	1 (384)	73 (2077)	12 (83)

*values in brackets indicate the total computational time in seconds.

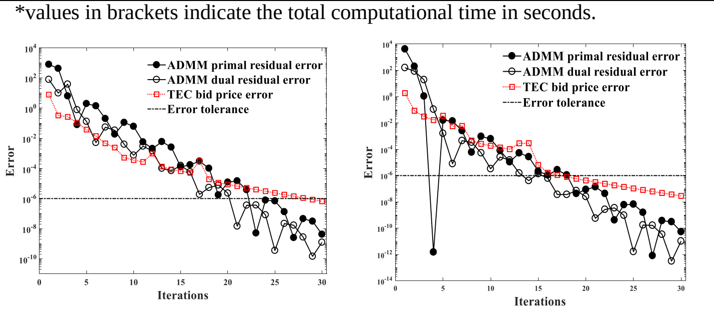

(a) SD (b) WD

Fig. 8. Evolution of convergence errors obtained by ADMM and bid price error obtained by TEC of grid-connected NMGs.

The interconnection network of NMGs can suffer from failures and congestion that constrain the energy transactions among NMGs. The congested mode is generated by constraining the maximum power flows among grid-connected NMGs to 500 kW. The optimized SD daily costs of all NMGs based on models M1 and M4 are \$1170.5 and \$1170.7, respectively. Compared to the results in Table V, the total daily cost increases due to the limited line capacities. The decentralized mechanism M2 is not simulated in the congested mode because individual MG operators may not have access to the congestion information in the interconnection network.

The daily LMP profiles at different NMGs with and without congestion obtained by the proposed model M4 are illustrated in Fig. 9. As can be seen in Fig. 9, the NMGs share an identical LMP curve based on the proposed model M4 when there is no congestion. However, their LMPs are quite different in congested mode. Moreover, to demonstrate the impact of congestion on proposed model M4, the changes in LMPs during the auction process at 10:00 on the SD are demonstrated in Figs. 10(a) and 10(b). From Fig. 10(a), LMPs at different MGs converge to the same value without congestion. In the congested mode, however, the LMPs of different NMGs also converge but not to the same value, as clearly illustrated in Fig. 10(b).

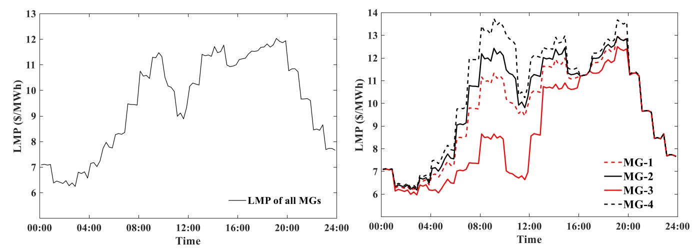

(a) no congestion (b) with congestion

Fig. 9. Comparison of daily LMP profiles of grid-connected NMGs on the SD with and without congestion based on the proposed TEC.

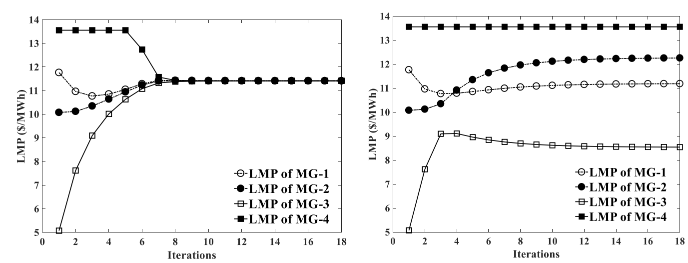

(a) no congestion (b) with congestion

Fig. 10. LMP profiles at 10:00 on the typical SD with and without congestion based on the proposed TEC.

C. Stochastic Operation Results

The generation outputs of RESs may suffer from significant oscillations and affect the collaborative trading among NMGs. Scenario-based stochastic optimization is employed in this subsection to verify the feasibility of the proposed TEC model M4 with respect to dealing with uncertain RESs.

The performance of the proposed TEC model M4 for stochastic NMG collaboration is verified in both grid-connected and islanded modes, with the results given in Table VIII. Compared to the results in Tables V and VI, the uncertainty of RESs will lead to higher daily energy costs. For grid-connected NMGs, the daily costs are slightly higher than reported in Tables V and VI thanks to support from ETS. On the other hand, the islanded NMGs suffer from higher RES curtailment and load shedding penalties due to the limited generation capabilities and the physical constraints of CGUs.

Table VIII also shows the results of model M4 when the fluctuations of RESs are more severe (i.e., the high and low forecasts are respectively 140% and 60% of the corresponding central forecast), with these optimized results given in brackets. The daily operating costs become even higher due to the increase in curtailment/shedding costs when the uncertainty of RESs grows larger.

TABLE VIII
PERFORMANCE OF PROPOSED TEC MODEL IN STOCHASTIC OPTIMIZATION

		Expected daily operating cost ($)	Expected daily curtailment/shedding cost ($)
SD	Grid-connected	1191.8 (1284.6)	0.0 (27.25)
	Islanded	1236.8 (1388.6)	0.0 (41.95)
WD	Grid-connected	2049.8 (2098.9)	0.0 (0.0)
	Islanded	2914.3 (3314.7)	808.7 (1250.4)

*values in brackets indicate the results with more severe RES fluctuations.

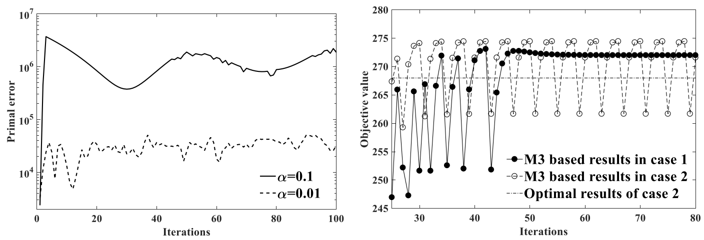

(a) results of M3 on the SD with ETS (b) convergence property of M3
Fig. 11. Convergence results of M3.

D. Discussion

The proposed models and case studies focus on the coordination of active power generation of CGUs and RESs among different NMGs. Because the models are developed based on proper relaxation and linearization of AC power flow constraints as discussed in Section III.A and Appendices A and B, the proposed models and methods can be further extended to accommodate the integration of other important factors such as collaborative reactive power optimization and demand response schemes, which will not be further discussed herein.

Based on the simulation results in the previous subsections, M1, M2, and the proposed M4 are all feasible for coordinating the deterministic and stochastic collaborative operation of NMGs. The proposed model M4 takes the least computational time in all grid-connected, islanded, and congested modes. Moreover, M1 suffers from unsatisfactory privacy protection and M2 requires an extra mechanism to monitor the status of the interconnection network so that issues related to the availability of the interconnection network, such as transmission congestion, can be dealt with. In addition, M4 enjoys better scalability than M1 and M2 since it can be processed in a distributed and parallel manner. As a result, the proposed TEC mechanism is shown to be an efficient and promising method to promote collaboration among NMGs.

The effectiveness of subgradient-based TEC model M3 is not illustrated in previous subsections because M3 fails to converge to feasible results. Fig. 11(a) demonstrates the primal errors of M3 for grid-connected NMGs on the SD in the first 100 iterations. The convergence errors of M3 clearly swing around 1e+6 and 1e+4 at step sizes of 0.1 and 0.01, respectively. While the ADMM-based M2 converges within a few tens of iterations with a step size of 0.1, M3 shows no signs of convergence in Fig. 11(a) and no feasible solution is obtained. When testing the effectiveness of subgradient-based TEC for islanded NMGs, the M3 model even becomes unbounded in the first two to three iterations. As a result, no feasible solutions can be obtained by solving M3 with the test case setup discussed in Section V.A.

A simplified test case with two MGs connected through a single line for a single operating time slot is adopted to achieve a converged example for M3. Fig. 11(b) illustrates the effectiveness of M3 in two cases. Constraint (2) is binding in case 1 and non-binding in case 2. As shown in Fig. 11(b), M3 converges to the optimal solution in case 1, but fails to converge and begins to oscillate in case 2. Thus, the subgradient-based TEC mechanism demonstrates poor convergence and should not be considered a viable solution to implement energy transactions and collaboration among NMGs.

VI. CONCLUSIONS

Coordination among NMGs through reasonable energy transactions is likely to minimize their global operating cost and enhance the utilization of renewable generation. This paper proposes a novel TEC model and a new pricing rule to facilitate collaboration, and compares this new approach to the centralized, decentralized, and subgradient-based TEC mechanisms. The effectiveness and computational efficiency of the proposed TEC mechanism in dealing with grid-connected, islanded, and congested NMGs in both deterministic and stochastic environments are verified through case studies.

Validated by case studies, the proposed TEC mechanism is able to accurately match the solutions of centralized mechanism while maintaining the MGs' privacy. Compared with the decentralized mechanism, the proposed TEC mechanism can be processed in parallel and takes less time to solve. Moreover, the proposed TEC does not suffer from convergence-related issues observed under subgradient-based methods. As a result, the proposed TEC mechanism is a promising solution to implement energy transactions and collaboration among NMGs.

APPENDIX

A. Centralized Optimization Model

The operational objective of the central system coordinator is to maximize its social welfare subject to AC power flow constraints. With the uncertainty modeled by the scenario-based stochastic optimization proposed in [31], the centralized optimization model can be described as:

$$\text{Min} \sum_{t\in\Omega_T} f_E(P_{E,t}) + \sum_{k\in\Omega_K}\sum_{t\in\Omega_T}\sum_{i\in\Omega_N} \rho^k (f_C(P_{i,t}^k) - f_U(P_{i,t}^k)) \tag{A1}$$

$$\text{s.t.} \quad P_{i,t}^k = P_{E,t} + P_{i,t}^{G,k} - P_{i,t}^D = \sum_{j\in\Omega_N} P_{ij,t}^k,\ \forall k\in\Omega_K \tag{A2}$$

$$Q_{i,t}^k = Q_{i,t}^{G,k} - Q_{i,t}^D = \sum_{j\in\Omega_N} Q_{ij,t}^k,\ \forall k\in\Omega_K \tag{A3}$$

$$P_{ij,t}^k = V_{i,t}^k V_{j,t}^k (G_{ij}\cos\theta_{ij,t}^k + B_{ij}\sin\theta_{ij,t}^k) - G_{ij}(V_{i,t}^k)^2,\ \forall k\in\Omega_K \tag{A4}$$

$$Q_{ij,t}^k = V_{i,t}^k V_{j,t}^k (G_{ij}\sin\theta_{ij,t}^k - B_{ij}\cos\theta_{ij,t}^k) + B_{ij}(V_{i,t}^k)^2,\ \forall k\in\Omega_K \tag{A5}$$

$$P_{i,t}^{G,\min} \le P_{i,t}^{G,k} \le P_{i,t}^{G,\max},\ \forall k\in\Omega_K \tag{A6}$$

$$Q_{i,t}^{G,\min} \le Q_{i,t}^{G,k} \le Q_{i,t}^{G,\max},\ \forall k\in\Omega_K \tag{A7}$$

$$P_i^{G,RD} \le P_{i,t}^{G,k} - P_{i,t-1}^{G,k} \le P_i^{G,RU},\ \forall k\in\Omega_K \tag{A8}$$

$$-P_{ij}^{\max} \le P_{ij,t}^k \le P_{ij}^{\max},\ \forall k\in\Omega_K \tag{A9}$$

$$V_i^{\min} \le V_{i,t}^k \le V_i^{\max},\ \forall k\in\Omega_K \tag{A10}$$

where $P_{i,t}^k$ and $Q_{i,t}^k$ denote the nodal active and reactive power injections at the *i*-th node and $P_{i,t}^{G,k}$, $Q_{i,t}^{G,k}$, $P_{i,t}^{D,k}$, and $Q_{i,t}^{D,k}$ denote the active and reactive power generation and consumption at the *i*-th node, respectively. $P_{ij,t}^k$ and $Q_{ij,t}^k$ denote the active and reactive power flow through line *i-j*, $V_{i,t}^k$ and $\theta_{ij,t}^k$ denote the voltage magnitude at the *i*-th node and the phase angle difference between the *i*-th and j-th nodes, respectively. G_{ij} and B_{ij} denote the real and imaginary parts of the nodal admittance matrix, respectively. $P_{i,t}^{G,\max}$, $P_{i,t}^{G,\min}$, $Q_{i,t}^{G,\max}$, and $Q_{i,t}^{G,\min}$ denote the maximum and minimum output of the active and reactive power of a generating unit at the i-th node, respectively. $P_i^{G,RU}$ and $P_i^{G,RD}$ denote the up and down ramping limit of the generating unit at the i-th node, respectively. $P_{ij}^{\max}$, $V_i^{\max}$, and $V_i^{\min}$ denote the line flow limit and voltage magnitude limits, respectively. Ω_N denotes the set of all nodes in the considered NMGs.

The objective function (A1) maximizes the social welfare of all the MGs. Constraints (A2) and (A3) represent the nodal power injection equations, and branch power flows are calculated by (A4) and (A5). Constraints (A6) and (A7) denote the active and reactive power generation limits, respectively. Constraint (A8) denotes the ramping limits of generating units. Constraints (A9) and (A10) represent the branch power flow limit and the nodal voltage magnitude limit, respectively.

B. Linearization of (2) and Zero Duality Gap Relaxation of (3)

The linearization method in [34] is employed to linearize the constraints of the NMG interconnection network (i.e., constraint (2)) while maintaining the information with respect to voltage magnitudes and transmission losses. The nonlinear AC power flow equations (A2)-(A5) are linearized as:

$$P_{E,t} + P_{i,t}^{G,k} - P_{i,t}^{D} = \sum_j P_{ij,t}^{k} + \frac{1}{2}\sum_j P_{ij,t}^{loss,k}\ , \forall k \in \Omega_K \tag{B1}$$

$$Q_{i,t}^{G,k} - Q_{i,t}^{D} = \sum_j Q_{ij,t}^{k} + \frac{1}{2}\sum_j Q_{ij,t}^{loss,k}\ , \forall k \in \Omega_K \tag{B2}$$

$$P_{ij,t}^{k} = -G_{ij}(V_{i,t}^{k} - V_{j,t}^{k}) + B_{ij}\theta_{ij,t}^{k}\ , \forall k \in \Omega_K \tag{B3}$$

$$Q_{ij,t}^{k} = B_{ij}(V_{i,t}^{k} - V_{j,t}^{k}) + G_{ij}\theta_{ij,t}^{k}\ , \forall k \in \Omega_K \tag{B4}$$

$$P_{ij,t}^{loss,k} \ge -G_{ij} f_d(\theta_{ij,t}^{k})\ ,\ \forall d \in [1,D], \forall k \in \Omega_K \tag{B5}$$

$$Q_{ij,t}^{loss,k} \ge B_{ij} f_d(\theta_{ij,t}^{k})\ ,\ \forall d \in [1,D], \forall k \in \Omega_K \tag{B6}$$

$$f_d(\theta_{ij,t}^{k}) = \chi_d \theta_{ij,t}^{k} + \beta_d\ ,\ \forall d \in [1,D], \forall k \in \Omega_K \tag{B7}$$

where $P_{ij,t}^{loss,k}$ and $Q_{ij,t}^{loss,k}$ denote the approximated active and reactive power losses of line i-j, respectively. f_d denotes the piecewise linearization function for power losses and D denotes the total number of piecewise linearization segments. χ_d and β_d denote the coefficients of the d-th linearization segment, respectively. The nonlinear power flow equations (A2)-(A5) are linearized as (B1)-(B4), respectively. The line losses are approximated by piecewise linearization function f_d as denoted in (B7). Constraints (B5) and (B6) are relaxed as inequality constraints so that the piecewise linearization of line losses does not require the introduction of binary variables.

To guarantee that the SOC relaxed constraint (3) has a zero duality gap, the method proposed in [36] is employed to relax the nodal injection equations (A2) and (A3) as follows:

$$P_{E,t} + P_{i,t}^{G,k} - P_{i,t}^{D} \ge \sum_j P_{ij,t}^{k}\ , \forall k \in \Omega_K \tag{B8}$$

$$Q_{i,t}^{G,k} - Q_{i,t}^{D} \ge \sum_j Q_{ij,t}^{u}\ , \forall k \in \Omega_K \tag{B9}$$

In this way, the relaxed constraint (3) has a zero duality gap, which means that the optimal value of the primal model equals that of the dual model [36]. Furthermore, the zero duality gap of constraint (3) satisfies the convergence and optimality criteria of ADMM [30]. Note that the relaxations (B8) and (B9) normally lead to optimal solutions identical to those based on unrelaxed (A2) and (A3) [36].

C. Proof of Theorem 1

Let L_1, $L_{4\text{-MG}}$, and $L_{4\text{-S}}$ denote the Lagrangians of M1, M4-MG, and M4-S, respectively. L_1, $L_{4\text{-MG}}$, and $L_{4\text{-S}}$ are respectively formulated as:

$$\begin{aligned} L_1 = \sum_{t\in\Omega_T} (\pi_{E,t}P_{E,t} + \sum_{k\in\Omega_K}\sum_{m\in\Omega_M} \rho^k (f_{C,m}(\mathbf{P}_{m,t}^k) - f_{U,m}(\mathbf{P}_{m,t}^k))) \\ + \boldsymbol{\lambda}^{\mathrm{T}}\mathbf{h}(P_{m,t}^{ex}, P_{E,t}) + \sum_{m\in\Omega_M} \boldsymbol{\mu}_{\mathbf{m}}^{\mathrm{T}}\mathbf{g}_{\mathbf{m}}(P_{m,t}^{ex}, \mathbf{P}_{m,t}^k) \end{aligned} \tag{C1}$$

$$\begin{aligned} L_{4\text{-MG}} = \sum_{t\in\Omega_T} (-\pi_{m,t}P_{m,t}^{ex} + \sum_{k\in\Omega_K} \rho^k (f_{C,m}(\mathbf{P}_{m,t}^k) - f_{U,m}(\mathbf{P}_{m,t}^k))) \\ + \boldsymbol{\tau}_{\mathbf{m}}^{\mathrm{T}}\mathbf{g}_{\mathbf{m}}(P_{m,t}^{ex}, \mathbf{P}_{m,t}^k) \end{aligned} \tag{C2}$$

$$L_{4\text{-S}} = \sum_{t\in\Omega_T} \pi_{E,t}P_{E,t}^{ex} + \sum_{t\in\Omega_T}\sum_{m\in\Omega_M} \pi_{m,t}P_{m,t}^{ex} + \boldsymbol{\sigma}^{\mathrm{T}}\mathbf{h}(P_{m,t}^{ex}, P_{E,t}) \tag{C3}$$

where $\boldsymbol{\lambda}$ and $\boldsymbol{\mu}_{\mathbf{m}}$ represent the Lagrange multipliers of M1, $\boldsymbol{\tau}_{\mathbf{m}}$ represents the Lagrange multipliers of M4-MG, and $\boldsymbol{\sigma}$ represents the Lagrange multiplier of M4-S.

The Karush-Kuhn-Tucker (KKT) conditions of M1, M4-MG, and M4-S are respectively demonstrated as:

$$\begin{cases} \nabla_{\mathbf{P}_{m,t}^k} L_1 = \rho^k(\nabla_{\mathbf{P}_{m,t}^k} f_{C,m} - \nabla_{\mathbf{P}_{m,t}^k} f_{U,m}) + \boldsymbol{\mu}_{\mathbf{m}}^{\mathrm{T}}\nabla_{\mathbf{P}_{m,t}^k}\mathbf{g}_{\mathbf{m}} = 0 \\ \nabla_{P_{E,t}} L_1 = \pi_{E,t} + \boldsymbol{\lambda}^{\mathrm{T}}\nabla_{P_{E,t}}\mathbf{h} = 0 \quad \mathbf{h}(P_{m,t}^{ex}, P_{E,t}) = 0 \\ \nabla_{P_{m,t}^{ex}} L_1 = \boldsymbol{\lambda}^{\mathrm{T}}\nabla_{P_{m,t}^{ex}}\mathbf{h} + \boldsymbol{\mu}_{\mathbf{m}}^{\mathrm{T}}\nabla_{P_{m,t}^{ex}}\mathbf{g}_{\mathbf{m}} = 0 \quad \mathbf{g}_{\mathbf{m}}(P_{m,t}^{ex}, \mathbf{P}_{m,t}^k) = 0 \end{cases} \tag{C4}$$

$$\begin{cases} \nabla_{\mathbf{P}_{m,t}^k} L_{4\text{-MG}} = \rho^k(\nabla_{\mathbf{P}_{m,t}^k} f_{C,m} - \nabla_{\mathbf{P}_{m,t}^k} f_{U,m}) + \boldsymbol{\tau}_{\mathbf{m}}^{\mathrm{T}}\nabla_{\mathbf{P}_{m,t}^k}\mathbf{g}_{\mathbf{m}} = 0 \\ \nabla_{P_{m,t}^{ex}} L_{4\text{-MG}} = -\pi_{m,t} + \boldsymbol{\tau}_{\mathbf{m}}^{\mathrm{T}}\nabla_{P_{m,t}^{ex}}\mathbf{g}_{\mathbf{m}} = 0 \quad \mathbf{g}_{\mathbf{m}}(P_{m,t}^{ex}, \mathbf{P}_{m,t}^k) = 0 \end{cases} \tag{C5}$$

$$\begin{cases} \nabla_{P_{E,t}} L_{4\text{-S}} = \pi_{E,t} + \boldsymbol{\sigma}^{\mathrm{T}}\nabla_{P_{E,t}}\mathbf{h} = 0 \\ \nabla_{P_{m,t}^{ex}} L_{4\text{-S}} = \pi_{m,t} + \boldsymbol{\sigma}^{\mathrm{T}}\nabla_{P_{m,t}^{ex}}\mathbf{h} = 0 \quad \mathbf{h}(P_{m,t}^{ex}, P_{E,t}) = 0 \end{cases} \tag{C6}$$

Let { $P_{E,t}^*$, $\mathbf{P}_{m,t}^{k*}$, $P_{m,t}^{ex*}$, $\boldsymbol{\lambda}^*$, $\boldsymbol{\mu}_{\mathbf{m}}^*$ } denote the optimal solution to M1. By constructing $\boldsymbol{\sigma} = \boldsymbol{\lambda}$ and $\boldsymbol{\tau}_{\mathbf{m}} = \boldsymbol{\mu}_{\mathbf{m}}$, { $P_{m,t}^{ex*}$, $\mathbf{P}_{m,t}^{k*}$, $\boldsymbol{\mu}_{\mathbf{m}}^*$ } obviously satisfies (C5) and { $P_{m,t}^{ex*}$, $P_{E,t}^*$, $\boldsymbol{\lambda}^*$ } satisfies (C6). Thus, the optimal solution to M1 solves M4-MG and M4-S and further solves M4.

Conversely, denote the optimal solution of M4-MG and M4-S as { $P_{m,t}^{ex\oplus}$, $\mathbf{P}_{m,t}^{k\oplus}$, $\boldsymbol{\tau}_{\mathbf{m}}^{\oplus}$ } and { $P_{m,t}^{ex\oplus}$, $P_{E,t}^{\oplus}$, $\boldsymbol{\sigma}^{\oplus}$ }, respectively. By constructing $\pi_{m,t}^{\oplus} = \boldsymbol{\tau}_{\mathbf{m}}^{\oplus\mathrm{T}}\nabla_{P_{m,t}^{ex\oplus}}\mathbf{g}_{\mathbf{m}}$ and substituting $\pi_{m,t}^{\oplus}$ into (C6), the following equation can be inferred:

$$\boldsymbol{\sigma}^{\oplus\mathrm{T}}\nabla_{P_{m,t}^{ex\oplus}}\mathbf{h} + \boldsymbol{\tau}_{\mathbf{m}}^{\oplus\mathrm{T}}\nabla_{P_{m,t}^{ex\oplus}}\mathbf{g}_{\mathbf{m}} = 0 \tag{C7}$$

Thus, { $P_{E,t}^{\oplus}$, $\mathbf{P}_{m,t}^{k\oplus}$, $P_{m,t}^{ex\oplus}$, $\boldsymbol{\sigma}^{\oplus}$, $\boldsymbol{\tau}_{\mathbf{m}}^{\oplus}$ } satisfies the KKT condition (C4), indicating that the optimal solution to M4 also solves M1. ■

D. Proof of Theorem 2

For the m-th MG, the optimal bidding price $\pi_{m,t}$ should satisfy the following KKT condition:

$$\nabla_{\pi_{m,t}} L_{4\text{-MG}} = 0 \tag{D1}$$

Based on the M4-MG model, (D1) can be represented as:

$$\begin{aligned} \nabla_{\pi_{m,t}} L_{4\text{-MG}} &= \frac{\partial L_{4\text{-MG}}}{\partial \pi_{m,t}} = \frac{\partial L_{4\text{-MG}}}{\partial P_{m,t}^{ex}}\frac{\partial P_{m,t}^{ex}}{\partial \pi_{m,t}} \\ &= (\frac{\partial f_{C,m}}{\partial P_{m,t}^{ex}} - \frac{\partial f_{U,m}}{\partial P_{m,t}^{ex}} + \frac{\partial f_S}{\partial P_{m,t}^{ex}} + \boldsymbol{\tau}_{\mathbf{m}}^{\mathrm{T}}\frac{\partial \mathbf{g}_{\mathbf{m}}}{\partial P_{m,t}^{ex}})\frac{\partial P_{m,t}^{ex}}{\partial \pi_{m,t}} = 0 \end{aligned} \tag{D2}$$

Referring to the definition of LMP, the LMP of active power injection from the m-th MG to the MG interconnection network can be expressed as:

$$\vartheta_{m,t} = \frac{\partial f_{C,m}}{\partial P_{m,t}^{ex}} - \frac{\partial f_{U,m}}{\partial P_{m,t}^{ex}} + \boldsymbol{\tau}_{\mathbf{m}}^{\mathrm{T}}\frac{\partial \mathbf{g}_{\mathbf{m}}}{\partial P_{m,t}^{ex}} \tag{D3}$$

Then (D4) can be inferred by substituting (D3) into (D2).

$$\nabla_{\pi_{m,t}} L_{4\text{-MG}} = (\frac{\partial f_S}{\partial P_{m,t}^{ex}} + \vartheta_{m,t})\frac{\partial P_{m,t}^{ex}}{\partial \pi_{m,t}} = 0 \tag{D4}$$

Equation (D5) can be derived by substituting (12) into (D4) so as to accommodate the KKT condition (D1):

$$\vartheta_{m,t} = -\frac{\partial f_S}{\partial P_{m,t}^{ex}} = \pi_{m,t} \tag{D5}$$

Although (D5) is explicit in deciding the bid price for NMGs, $\vartheta_{m,t}$ cannot be directly used as bid prices because $\vartheta_{m,t}$ is related to $\Delta P_{m,t}^{ex(r)}$, which is unknown to the MG operator before the system coordinator clears the *r*-th round energy transactions. Alternatively, $\vartheta_{m,t}$ can be expressed as the linear function shown in (D6) based on assumption (ii):

$$\vartheta_{m,t} = \omega_1 P_{m,t}^{ex} + \omega_2 \tag{D6}$$

where ω_1 and ω_2 are coefficients.

Coefficient ω_1 denotes the equivalent leading coefficient of all marginal units under all possible scenarios. Because the marginal generating units share the same marginal generation cost in every scenario, a marginal increment in $P_{m,t}^{ex(r)}$ will be allocated to each marginal unit according to the following rule:

$$\alpha_j^k \Delta P_j^k = C_{m,t} \ , \forall j \in \Omega_{m,t} \ , \forall k \in \Omega_K \tag{D7}$$

where $C_{m,t}$ is a constant number and ΔP_j^k is the proportion of power increment allocated to the *j*-th marginal generating unit in the *k*-th scenario. Then, ω_1 can be calculated as:

$$\omega_1 = \sum_{k \in \Omega_K} \rho^k \left(\sum_{j \in \Omega_{m,t}} \frac{1}{\alpha_j + \varepsilon} \right)^{-1} \tag{D8}$$

Considering the *r*-th round energy transaction bidding, the individual MG operators only have the information of $P_{m,t}^{ex(r-1)}$ and $\vartheta_{m,t}^{(r-1)}$ when deciding $\pi_{m,t}^{(r)}$. By substituting (13) and (D6) into (D5), $\vartheta_{m,t}^{(r)}$ is calculated as:

$$\begin{aligned} \vartheta_{m,t}^{(r)} &= \omega_1 P_{m,t}^{ex(r)} + \omega_2 = \omega_1 (P_{m,t}^{ex(r-1)} + \Delta P_{m,t}^{ex(r)}) + \omega_2 \\ &= \omega_1 \Delta P_{m,t}^{ex(r)} + \vartheta_{m,t}^{(r-1)} \end{aligned} \tag{D9}$$

By selecting the coefficient $\varpi_{m,t} = \omega_1$ and substituting (D5) into (D9), the optimal bid price $\pi_{m,t}^{(r)}$ is formulated as:

$$\pi_{m,t}^{(r)} = \vartheta_{m,t}^{(r)} = \omega_1 \Delta P_{m,t}^{ex(r)} + \vartheta_{m,t}^{(r-1)} = \varpi_{m,t} \Delta P_{m,t}^{ex(r)} + \vartheta_{m,t}^{(r-1)} \tag{D10}$$

Thus, the proposed bidding strategy (14) becomes identical to (D10), which further satisfies the KKT condition of the optimal bidding price in (D1). Therefore, the optimality of the proposed pricing rule (14) is proven. ■

REFERENCES

[1] N. Hatziagyriou, H. Asano, R. Iravani, and C. Marnay, "Microgrids: an overview of ongoing research, development and demonstration projects," *IEEE Power Energy Mag.*, vol. 5, no. 4, pp. 78-94, Jul./Aug. 2007.

[2] A. Q. Huang, M. L. Crow, G. T. Heydt, J. P. Zheng, and S. J. Dale, "The future renewable electric energy delivery and management (FREEDM) system: the energy internet," *Proc. IEEE*, vol. 99, no. 1, pp. 133-148, Jan. 2011.

[3] T. A. Nguyen and M. L. Crow, "Stochastic optimization of renewable-based microgrid operation incorporating battery operating cost," *IEEE Trans. Power Syst.*, vol. 31, no. 3, pp. 2289-2296, May 2016.

[4] A. Khodaei, "Microgrid optimal scheduling with multi-period islanding constraints," *IEEE Trans. Power Syst.*, vol. 29, no. 4, pp. 1383-1392, May 2014.

[5] M. Shahidehpour, Z. Li, S. Bahramirad, Z. Li, and W. Tian, "Networked microgrids: Exploring the possibilities of the IIT-bronzeville grid," *IEEE Power Energy Mag.*, vol. 15, no. 4, pp. 63-71, Jul./Aug. 2017.

[6] Z. Wang, B. Chen, J. Wang, and C. Chen, "Networked microgrids for self-healing power systems," *IEEE Trans. Smart Grid*, vol. 7, no. 1, pp. 310-319, Jan. 2016.

[7] Z. Li, M. Shahidehpour, F. Aminifar, A. Alabdulwahab, and Y. Al-Turki, "Networked microgrids for enhancing the power system resilience," *Proc. IEEE*, vol. 105, no. 7, pp. 1289-1310, Jul. 2017.

[8] Canadian Wind Energy Association, "Wind data," [Online]. Available: https://canwea.ca/wind-integration-study/wind-data/

[9] Natural Resources Canada, "Solar resource data available for Canada," [Online]. Available: http://www.nrcan.gc.ca/energy/renewable-electricity /solar-photovoltaic/14390

[10] M. R. Sandgani and S. Sirouspour, "Coordinated optimal dispatch of energy storage in a network of grid-connected microgrids," *IEEE Trans. Sustain. Energy*, vol. 8, no. 3, pp. 1166-1176, Jul. 2017.

[11] Z. Wang, B. Chen, J. Wang, M. M. Begovic, and C. Chen, "Coordinated energy management of networked microgrids in distribution systems," *IEEE Trans. Smart Grid*, vol. 6, no. 1, pp. 45-53, Jan. 2015.

[12] G. E. Asimakopoulou, A. L. Dimeas, and N. D. Hatziargyriou, "Leader-follower strategies for energy management of multi-microgrids," *IEEE Trans. Smart Grid*, vol. 4, no. 4, pp. 1909-1916, Dec. 2013.

[13] A. R. Malekpour and A. Pahwa, "Stochastic networked microgrid energy management with correlated wind generators," *IEEE Trans. Power Syst.*, vol. 32, no. 5, pp. 3681-3693, Sep. 2017.

[14] Z. Wang, B. Chen, J. Wang, and J. Kim, "Decentralized energy management system for networked microgrids in grid-connected and islanded modes," *IEEE Trans. Smart Grid*, vol. 7, no. 2, pp. 1097-1105, Mar. 2016.

[15] H. K. Nguyen, A. Khodaei, and Z. Han, "Incentive mechanism design for integrated microgrids in peak ramp minimization problem," *IEEE Trans. Smart Grid*, early access.

[16] Z. Miao and L. Fan, "A novel multi-agent decision making architecture based on dual's dual problem formulation," *IEEE Trans. Smart Grid*, vol. 9, no. 2, pp. 1150-1160, Mar. 2018.

[17] K. Kok and S. Widergren, "A society of devices: integrating intelligent distributed resources with transactive energy," *IEEE Power & Energy Mag.*, vol. 14, no. 3, pp. 34-45, May/Jun. 2016.

[18] J. Hu, G. Yang, K. Kok, Y. Xue, and H. W. Bindner, "Transactive control: a framework for operating power systems characterized by high penetration of distributed energy resources," *J. Mod. Power Syst. Clean Energy*, vol. 5, no. 3, pp. 451-464, May 2017.

[19] H. Wang and J. Huang, "Incentivizing energy trading for interconnected microgrids," *IEEE Trans. Smart Grid*, vol. 9, no. 4, pp. 2647-2657, Jul. 2018.

[20] N. Liu, X. Yu, C. Wang, C. Li, L. Ma, and J. Lei, "Energy-sharing model with price-based demand response for microgrids of peer-to-peer prosumers," *IEEE Trans. Power Syst.*, vol. 32, no. 5, pp. 3569-3583, Sep. 2017.

[21] G. E. Rahi, S. R. Etesami, W. Saad, N. Mandayam, and H. V. Poor, "Managing price uncertainty in prosumer-centric energy trading: a prospect-theoretic Stackelberg game approach," *IEEE Trans. Smart Grid*, early access.

[22] T. Morstyn and M. D. McCulloch, "Multi-class energy management for peer-to-peer energy trading driven by prosumer preferences," *IEEE Trans. Power Syst.*, early access.

[23] Y. Amanbek, Y. Tabarak, H. S. V. S. K. Nunna, and S. Doolla, "Decentralized transactive energy management system for distribution systems with prosumer microgrids," in *19th International Carpathian Control Conference*, Szilvásvárad, Hungary, May 2018, pp. 553-558.

[24] M. S. Nazir and I. A. Hiskens, "A dynamical systems approach to modeling and analysis of transactive energy coordination," *IEEE Trans. Power Syst.*, early access.

[25] S. Weckx, R. D'Hulst, B. Claessens, and J. Driesen, "Multiagent charging of electric vehicles respecting distribution transformer loading and voltage limits," *IEEE Trans. Smart Grid*, vol. 5, no. 6, pp. 2857-2867, Nov. 2014.

[26] M. Fathi and H. Bevrani, "Statistical cooperative power dispatching in interconnected microgrids," *IEEE Trans. Sustain. Energy*, vol. 4, no. 3, pp. 586-593, Jul. 2013.

[27] D. Gregoratti and J. Matamoros, "Distributed energy trading: the multiple-microgrid case," *IEEE Trans. Ind. Electron.*, vol. 62, no. 4, pp. 2551-2559, Apr. 2015.

[28] J. Kang, R. Yu, X. Huang, S. Maharjan, Y. Zhang, and E. Hossain, "Enabling localized peer-to-peer electricity trading among plug-in hybrid electric vehicles using consortium blockchains," *IEEE Trans. Ind. Inform.*, vol. 13, no. 6, pp. 3154-3164, Dec. 2017.

[29] B. P. Majumder, M. N. Faqiry, S. Das, and A. Pahwa, "An efficient iterative double auction for energy trading in microgrids," in *2014 IEEE Symposium on Computational Intelligence Applications in Smart Grid*, Orlando, FL, USA, Dec. 2014.

[30] S. Boyd, N. Parikh, E. Chu, B. Peleato, and J. Eckstein, "Distributed optimization and statistical learning via the alternating direction method and multipliers," *Foundations and Trends in Machine Learning*, vol. 3, no. 1, pp. 1-122, Jan. 2011.

[31] J. M. Morales, A. J. Conejo, and J. Perez-Ruiz, "Economic valuation of reserves in power systems with high penetration of wind power," *IEEE Trans. Power Syst.*, vol. 24, no. 2, pp. 900-910, May 2009.

[32] S. Boyd and L. Vandenberghe, Convex Optimization. Cambridge Univ. Press, 2004.

[33] R. A. Jabr, R. Singh, and B. C. Pal, "Minimum loss network recon-figuration using mixed-integer convex programming," *IEEE Trans. Power Syst.*, vol. 27, no. 2, pp. 1106-1115, May 2012.

[34] H. Zhang, G. T. Heydt, V. Vittal, and J. Quintero, "An improved network model for transmission expansion planning considering reactive power and network losses," *IEEE Trans. Power Syst.*, vol. 28, no. 3, pp. 3471-3479, Aug. 2013.

[35] C. Feng, Z. Li, M. Shahidehpour, F. Wen, W. Liu, and X. Wang, "Decentralized short-term voltage control in active power distribution systems," *IEEE Trans. Smart Grid*, early access.

[36] J. Lavaei and S. H. Low, "Zero duality gap in optimal power flow problem," *IEEE Trans. Power Syst.*, vol. 27, no. 1, pp. 92-107, Feb. 2012.

[37] D. P. Bertsekas, *Convex Analysis and Optimization*. Nashua, NH, USA: Athena Scientific, 2003.

[38] H. Pandzic, Y. Dvorkin, T. Qiu, Y. Wang, and D. S. Kirschen, "Toward cost-efficient and reliable unit commitment under uncertainty," *IEEE Trans. Power Syst.*, vol. 31, no. 2, pp. 970-982, March 2016.

[39] Y. Wen, W. Li, G. Huang, and X. Liu, "Frequency dynamics constrained unit commitment with battery energy storage," *IEEE Trans. Power Syst.*, vol. 31, no. 6, pp. 5115-5125, Nov. 2016.

[40] J. Zhan, C. Y. Chung, and A. Zare, 'A fast solution method for stochastic transmission expansion planning,' *IEEE Trans. Power Syst.*, vol. 32, no. 6, pp. 4684-4695, Nov. 2017.

Weijia Liu received the B.Eng. and Ph.D. degrees in electrical engineering from Zhejiang University, Hangzhou, China, in 2011 and 2016, respectively.

He is currently a Postdoctoral Fellow in the Department of Electrical and Computer Engineering, University of Saskatchewan, Saskatoon, SK, Canada.

Junpeng Zhan (M'16) received the B.Eng. and Ph.D. degrees in electrical engineering from Zhejiang University, Hangzhou, China, in 2009 and 2014, respectively.

He is currently a Research Associate Electrical Engineer in the Sustainable Energy Technologies Department, Brookhaven National Laboratory, Upton, NY, USA. He was a Postdoctoral Fellow in the Department of Electrical and Computer Engineering, University of Saskatchewan, Saskatoon, SK, Canada.

C. Y. Chung (M'01-SM'07-F'16) received the B.Eng. (with First Class Honors) and Ph.D. degrees in electrical engineering from The Hong Kong Polytechnic University, Hong Kong, China, in 1995 and 1999, respectively.

He is currently a Professor and the SaskPower Chair in Power Systems Engineering in the Department of Electrical and Computer Engineering at the University of Saskatchewan, Saskatoon, SK, Canada.

Dr. Chung is an Editor of *IEEE Transactions on Power Systems*, *IEEE Transactions on Sustainable Energy*, and *IEEE Power Engineering Letters*. He is also a Member-at-Large (Global Outreach) of the IEEE PES Governing Board.